Bioorganic Chemistry 93 (2019) 103300

Contents lists available at ScienceDirect

Bioorganic Chemistry

journal homepage: www.elsevier.com/locate/bioorg

Design, synthesis and biological evaluation of flexible and rigid analogs of 4*H*-1,2,4-triazoles bearing 3,4,5-trimethoxyphenyl moiety as new antiproliferative agents

Mahsa Ansari[a], Mohammad Shokrzadeh[b], Saeed Karima[c], Shima Rajaei[c], Seyedeh Mahdieh Hashemi[d], Hassan Mirzaei[a], Marjan Fallah[b], Saeed Emami[d,*]

[a] Pharmaceutical Sciences Research Center, Student Research Committee, Faculty of Pharmacy, Mazandaran University of Medical Sciences, Sari, Iran
[b] Department of Toxicology and Pharmacology, Faculty of Pharmacy, Mazandaran University of Medical Sciences, Sari, Iran
[c] Department of Clinical Biochemistry, School of Medicine, Shahid Beheshti University of Medical Sciences (SBMU), Tehran, Iran
[d] Department of Medicinal Chemistry and Pharmaceutical Sciences Research Center, Faculty of Pharmacy, Mazandaran University of Medical Sciences, Sari, Iran

ARTICLE INFO

Keywords:
Anticancer agents
4*H*-1,2,4-triazoles
Cytotoxic activity
3,4,5-trimethoxyphenyl
Conformationally constrained

ABSTRACT

Several flexible and rigid analogs of 4*H*-1,2,4-triazoles (compounds **8a-g** and **9a-g**) bearing trimethoxyphenyl pharmacophoric unit, were designed and synthesized as potential anticancer agents. The in vitro cytotoxic assay indicated that both flexible and rigid analogs (**8** and **9**, respectively) can potentially inhibit the growth of cancerous cells (A549, MCF7, and SKOV3), with IC_{50} values less than 5.0 μM. Furthermore, compounds **10a-l** as regional isomers of compounds **9** exhibited remarkable cytotoxic activity with IC_{50} values ranging from 0.30 to 5.0 μM. The rigid analogs **9a**, **10h** and **10k** were significantly more potent than etoposide against MCF7, SKOV3 and A549 cells, respectively. These compounds showed high selectivity towards cancer cells over normal cells, as they had no significant cytotoxicity against L929 cells. In addition, the representative compounds **9a** and **10h** could inhibit the tubulin polymerization at micro-molar levels. By determining changes in the colchicine-tubulin fluorescence, it was suggested that compound **10h** could bind to the tubulin at the colchicine pocket. The molecular docking study further confirmed the inhibitory activity of promising compounds **9a**, **10h** and **10k** on tubulin polymerization through binding to the colchicine-binding site.

1. Introduction

Cancers are characterized by the uncontrolled growth and spread of abnormal cells awfully threat human life. Although several drugs have been introduced to treat these diseases, but most of the prevalent types of cancers are regrettably still uncontrolled [1]. Furthermore, it seems that the most of anticancer agents which targeting a single protein or enzyme are unsuccessful in treating cancer cells, due to the high incidence of resistance [2]. Hence, discovery and development of new effective anticancer drugs with diverse mechanism of actions is required.

Previous studies have been shown that trimethoxyphenyl moiety acts as a pharmacophoric group for the anticancer effect of some natural anticancer compounds such as colchicine (**1**, Fig. 1), combretastatin (**2**), podophyllotoxin (**3**), and poly-methoxychalcone (**4**) [3–6]. Mechanistically, these compounds were found to be tubulin inhibitors, which bind to the colchicine-binding site, leading to microtubule depolymerization. Microtubules have critical roles in several cellular processes, particularly in mitosis. Therefore, microtubules have been considered as an attractive target for anticancer drug discovery [7]. Although trimethoxyphenyl based anticancer agents have recently gained great successes, however none of these natural-derived compounds have been approved by FDA to be marketed as anticancer drug. Several drawbacks including metabolic instability, low oral bioavailability, poor aqueous solubility and undesired side effects have hindered the development of this type of compounds [8].

The introduction of a proper heterocycle in the structure of trimethoxyphenyl-based compounds would be a good strategy to overcome some of mentioned problems [9]. Among the various heterocycles studied, the triazole nucleus has been attracted much attention in recent years, due to its metabolic stability, good solubility, and capability for hydrogen bonding [10]. For example, Romagnoli et al. have reported trimethoxyphenyl-based 5-amino-1,2,4-triazoles as potent antimitotic agents. Among them, compound **5** (Fig. 1) was the most potent

* Corresponding author.
E-mail addresses: semami@mazums.ac.ir, sdemami12@gmail.com (S. Emami).

https://doi.org/10.1016/j.bioorg.2019.103300
Received 28 June 2019; Received in revised form 15 September 2019; Accepted 16 September 2019
Available online 21 September 2019
0045-2068/

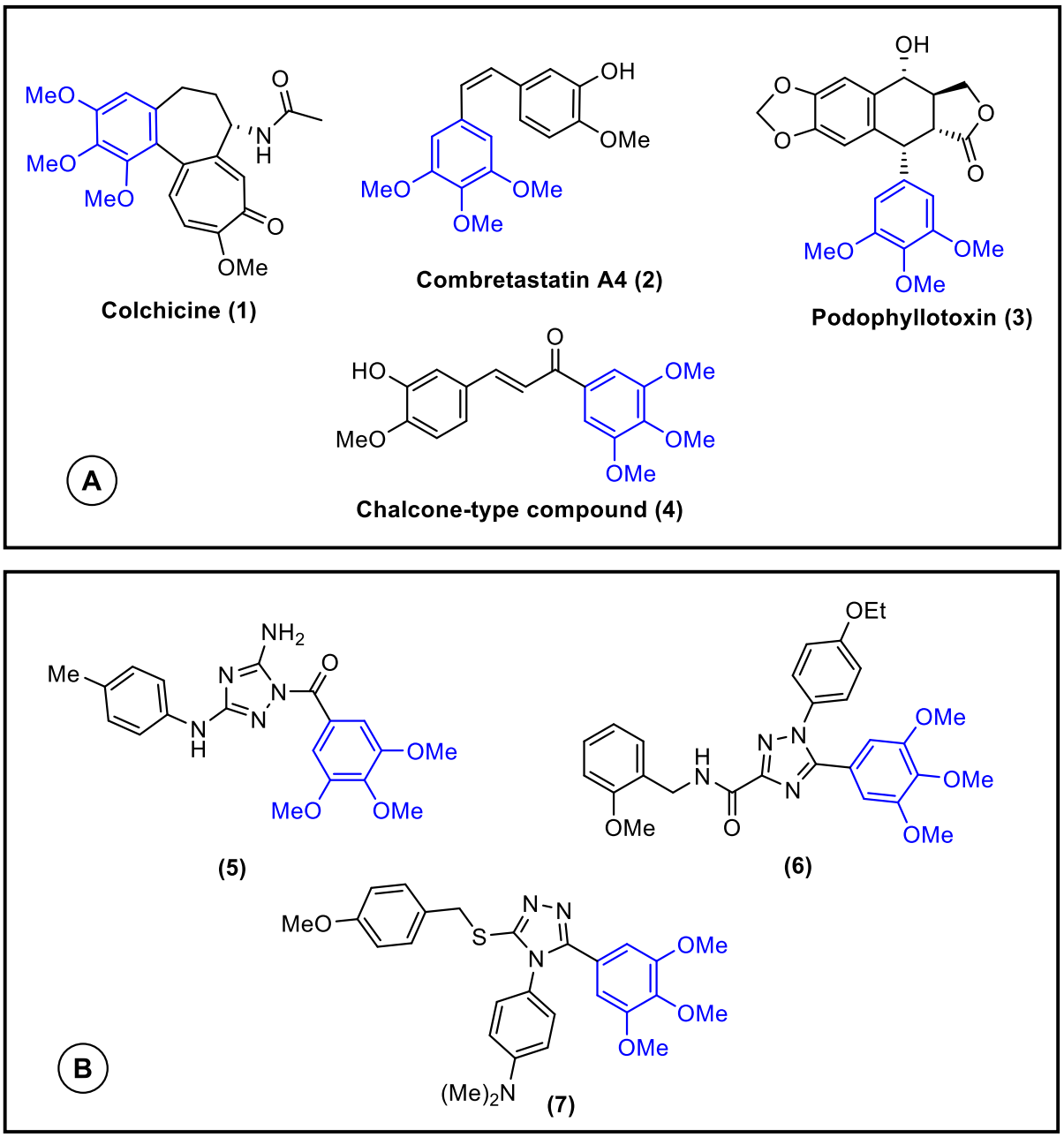

Fig. 1. Structures of some anti-cancer agents containing trimethoxyphenyl moiety: (A) natural anticancers; (B) triazole-derived synthetic compounds.

compound with IC_{50} values of 0.21 and 3.2 nM against CEM and Hela cells, respectively [11].

A series of 1,2,4-triazole-3-carboxamide derivatives were designed and synthesized as potent combretastatin analogs by Mustafa and coworkers. The cytotoxicity assay revealed that compound **6** was more potent than combretastatin against HepG2 cells. This compound also significantly inhibited the growth of MOLT-4, SK-MEL-5, and UO-31 cancer cells in NCI60 assay [12]. In another study, several 3-(benzylthio)-4*H*-1,2,4-triazoles bearing trimethoxyphenyl scaffold were synthesized and tested against different cell lines. Compound **7** showed IC_{50} value of 1.15 μM against HCT116 cells, being five times more potent than combretastatin [13].

In continuation of our work on the heterocyclic anticancer agents containing trimethoxyphenyl moiety [14], we have designed and synthesized 4-amino-5-aryl-4*H*-1,2,4-triazoles **8** (Fig. 2) bearing 3,4,5-trimethoxy-phenacylthio residue. These compounds can be considered as chalcone-like compounds which the 4-amino-3-thio-4*H*-1,2,4-triazole was inserted in their structure. Cyclization of the flexible analogs **8** resulted in rigid congeners **9** with a triazolothiadiazine framework. Further displacement of trimethoxy substituent led to regional isomers **10**. Thus, we report here, the synthesis, biological evaluation and molecular modeling of compounds **8–10** as anticancer agents (Fig. 2).

2. Results and discussion

2.1. Chemistry

The target compounds **8–10** were synthesized by employing reaction sequences outlined in Schemes 1 and 2. Firstly, the α-bromination of 3,4,5-trimethoxyacetophenone (**11a**) was conducted by using $CuBr_2$ in refluxing $CHCl_3$-EtOAc to give corresponding α-bromo compound **12a**. The reaction of compound **12a** with desired 3-mrecapto-4-

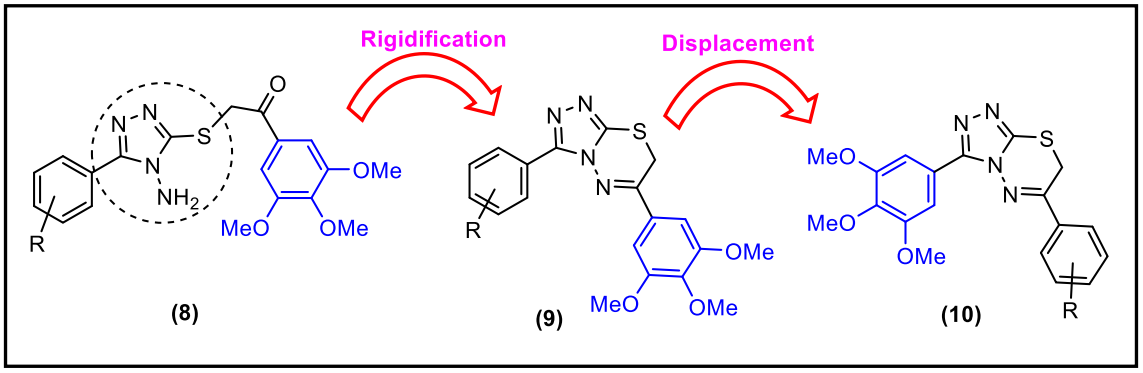

Fig. 2. Structures of designed compounds **8–10**.

aminotriazoles **13**, in the presence of K_2CO_3 as a base in dry acetone, at room temperature gave exclusively the *S*-phenacyl derivatives **8a-g**. The synthesis of intermediates **13** were reported previously by us [15,16]. When the reaction of α-bromo compound **12a** and 3-mrecapto-4-aminotriazoles **13** was conducted in refluxing absolute EtOH, the cyclized analogs **9a-g** were directly obtained as pure products. Furthermore, the annulated triazoles **9a-g** were obtained by refluxing of compounds **8a-g** in absolute ethanol. In order to investigate the importance of trimethoxyphenyl moiety in the SAR study, a couple of monomethoxy compounds (**9h** and **9i**) were also synthesized by same way, as illustrated in Scheme 1.

For preparation of the retro-analogs of **9** namely compounds **10**, the inversely substituted intermediates **17** and **12a-l** were used as presented in Scheme 2. Thus, the ethyl ester derivative **14** was converted to acid hydrazide **15** by treating with hydrazine hydrate 80%. The reaction of acid hydrazide **15** with carbon disulfide in the presence of potassium hydroxide in absolute ethanol at room temperature resulted in potassium dithioate salt **16**, which in next step refluxed with hydrazine hydrate until the color of the solution became clear green. Neutralization of the latter reaction mixture with 3 N hydrochloric acid, gave pure

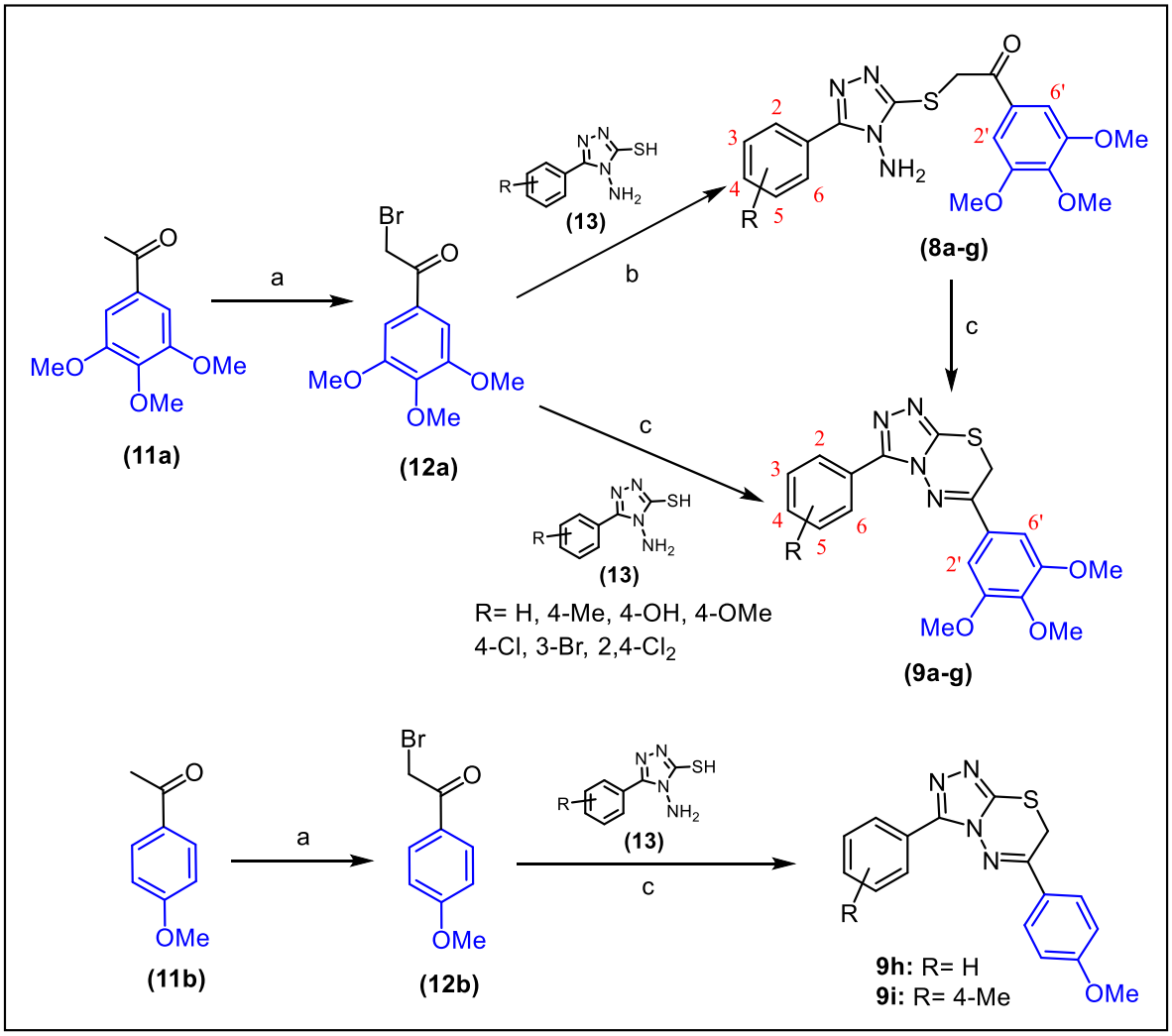

Scheme 1. Synthesis of compounds **8** and **9**. *Reagents and conditions*: (a) $CuBr_2$, $CHCl_3$-EtOAC, reflux; (b) K_2CO_3, dry acetone, rt; (c) absolute EtOH, reflux.

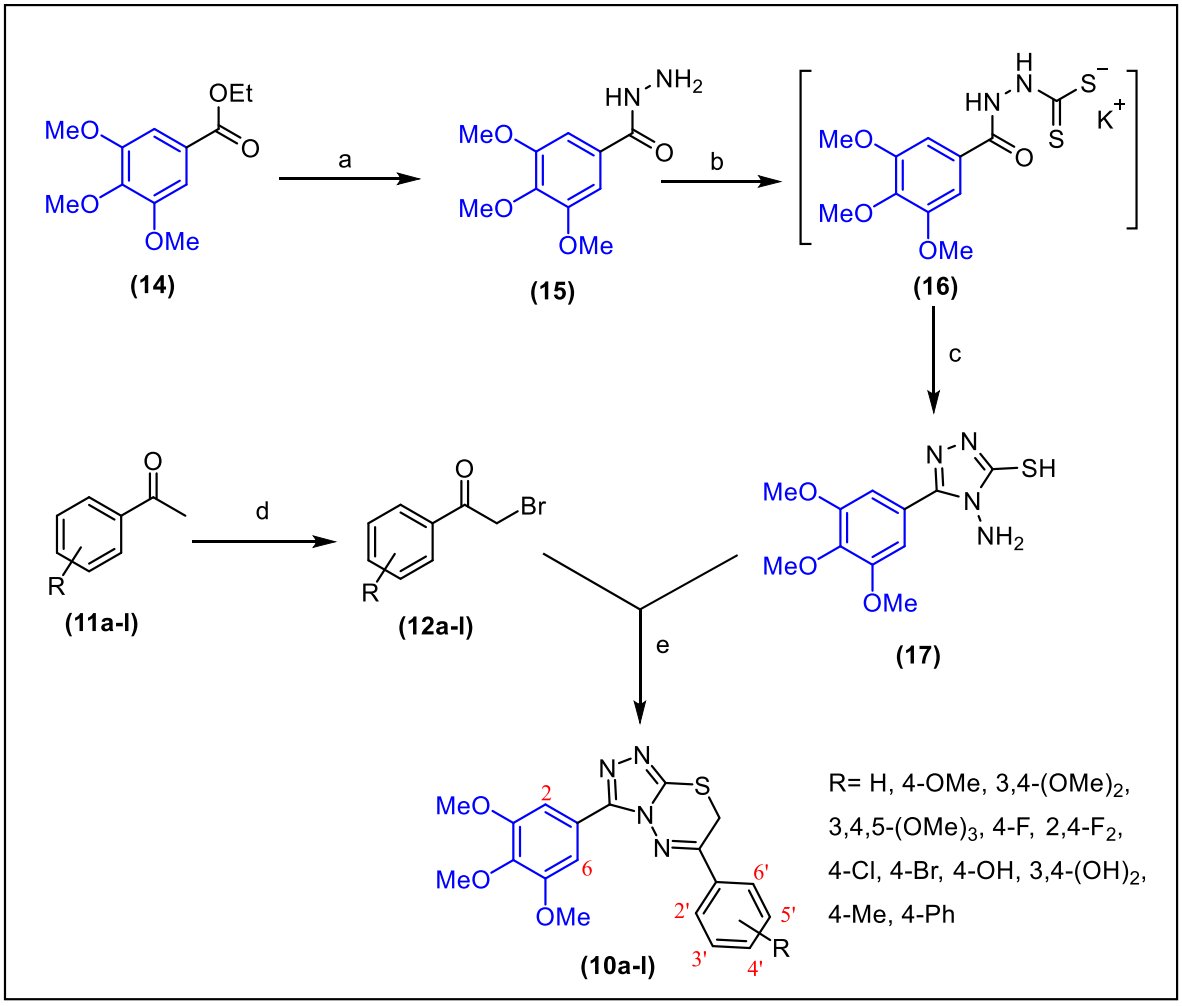

Scheme 2. Synthesis of compounds **10a-l**. *Reagents and conditions*: (a) $NH_2NH_2{\cdot}H_2O$ 80%; (b) CS_2, KOH, EtOH, rt; (c) $NH_2NH_2{\cdot}H_2O$ 80%, reflux, then HCl; (d) $CuBr_2$, $CHCl_3$-EtOAC, reflux; (e) absolute EtOH, reflux.

3-mrecapto-4-aminotriazole **17**. Finally, different phenacyl bromides **12a-l** were treated with *S,N*-nucleophile **17** in refluxing EtOH to afford triazolothiadiazine derivatives **10a-l**.

2.2. Biological activity

2.2.1. Anti-proliferative activity against cancer cell lines

The in vitro anti-proliferative activity of synthesized compounds **8–10** against three human cancer cell lines including adenocarcinomic human alveolar basal epithelial cells (A549), breast cancer cells (MCF7), and human ovarian carcinoma cells (SKOV3) was evaluated by using standard MTT assay as described earlier [17]. Etoposide was chosen as standard drug. Cytotoxic activities against different cancer cell lines are expressed as IC_{50} values (the concentration causing 50% inhibition of cell growth) in Tables 1 and 2.

As evidenced by data, both acyclic aminotriazoles **8a-g** and fused bicyclic triazoles **9a-g** and **10a-l** showed potent cytotoxic activity against tested cancer cell lines (IC_{50} values < 5.0 μM). In all trimethoxyphenyl series, we could find promising compounds with equal or superior activity compared to reference drug etoposide. For example, the 3-bromophenyl derivative **8d** from aminotriazole series exhibited IC_{50} value of 0.36 μM against SKOV3 cells, which was 6 times more potent than etoposide. Interestingly, the direct cyclic analog of **8d** (compound **9d**) was found to be the most active compound against A549 cells (IC_{50} = 0.67 μM), which was 4-fold more potent than etoposide. In the case of MCF7 cells, the unsubstituted compound **9a** with

Table 1
Anti-proliferative activity (IC_{50}, μM) of acyclic analogs **8a-g** in comparison with standard drug etoposide.*

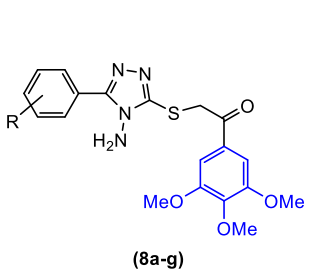

(8a-g)

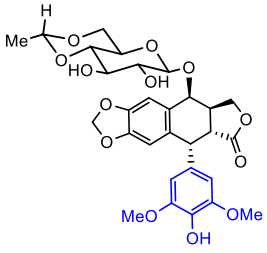

Etoposide

Compound	R	A549	MCF-7	SKOV3
8a	H	3.95 ± 0.17	3.70 ± 0.06	5.00 ± 0.17
8b	4-Me	4.39 ± 0.19	3.81 ± 0.06	3.55 ± 0.14
8c	4-OH	4.20 ± 0.06	4.61 ± 0.10	3.58 ± 0.19
8d	3-Br	3.67 ± 0.07	4.05 ± 0.21	0.36 ± 0.25
8e	4-OMe	2.58 ± 0.03	3.32 ± 0.09	2.68 ± 0.40
8f	4-Cl	2.81 ± 0.16	2.35 ± 0.11	1.29 ± 0.18
8g	2,4-Cl_2	3.79 ± 0.29	2.47 ± 0.17	0.71 ± 0.39
Etoposide		2.99 ± 0.18	1.89 ± 0.12	2.30 ± 0.17

* IC_{50} values are indicated as the mean ± SD of three independent experiments.

Table 2
Anti-proliferative activity (IC_{50}, μM) of rigid compounds **9a-i** and **10a-l**.*

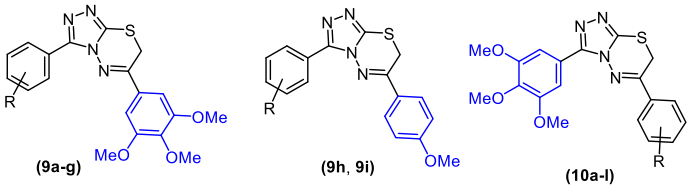

Compound	R	A549	MCF-7	SKOV3
9a	H	3.71 ± 0.13	0.70 ± 0.04	4.63 ± 0.09
9b	4-Me	4.57 ± 0.17	4.94 ± 0.05	2.85 ± 0.16
9c	4-OH	4.17 ± 0.17	2.43 ± 0.14	0.92 ± 0.08
9d	3-Br	0.67 ± 0.28	2.26 ± 0.20	3.91 ± 0.19
9e	4-OMe	3.20 ± 0.15	1.79 ± 0.03	2.20 ± 0.11
9f	4-Cl	3.94 ± 0.14	1.53 ± 0.19	4.20 ± 0.15
9g	2,4-Cl_2	2.73 ± 0.13	2.37 ± 0.15	3.95 ± 0.16
9h	H	> 5.0	> 5.0	Not tested
9i	4-Me	> 5.0	> 5.0	> 5.0
10a	H	1.04 ± 0.04	2.74 ± 0.28	4.00 ± 0.42
10b	4-OMe	3.6 ± 0.05	2.62 ± 0.24	3.00 ± 0.38
10c	3,4-$(OMe)_2$	2.5 ± 0.04	4.18 ± 0.31	4.41 ± 0.44
10d	3,4,5-$(OMe)_3$	4.0 ± 0.05	3.79 ± 0.04	2.18 ± 0.49
10e	4-F	2.8 ± 0.06	3.17 ± 0.01	4.90 ± 0.35
10f	2,4-F_2	2.15 ± 0.02	4.25 ± 0.03	3.74 ± 0.28
10g	4-Cl	4.97 ± 0.03	3.82 ± 0.01	4.71 ± 0.32
10h	4-Br	3.15 ± 0.01	3.34 ± 0.02	0.30 ± 0.65
10i	4-OH	5.01 ± 0.05	1.25 ± 0.01	3.98 ± 0.36
10j	3,4-$(OH)_2$	3.23 ± 0.27	1.52 ± 0.29	4.63 ± 0.34
10k	4-Me	0.60 ± 0.02	2.75 ± 0.05	3.43 ± 0.33
10l	4-Ph	4.01 ± 0.03	2.40 ± 0.04	2.67 ± 0.41
Etoposide		2.99 ± 0.22	1.89 ± 0.16	2.30 ± 0.12

* IC_{50} values are indicated as the mean ± SD of three independent experiments.

IC_{50} value of 0.7 μM showed the greatest potency among the tested compounds.

A survey on the structures and activities in Table 2 revealed that the IC_{50} values of compounds with different substituents are relatively close together, which indicates the intrinsic cytotoxic potential of designed framework. The effect of substituent on the cytotoxic activity depends on the type of tested cell line. For example, the comparison of unsubstituted compound **9a** and 3-bromo derivative **9d** reveals that the introduction of 3-bromo group improves the activity against A549 cell while diminishes the activity towards MCF7 cells. With these results in hand, it seems that the physicochemical and ADME-Tox properties of compounds can be optimized while cytotoxic activity of compounds is maintained.

Surprisingly, there are no dramatic differences between the range of IC_{50}s in acyclic derivatives **8a-g** and their rigid analogs **9a-g**. Furthermore, by comparing compounds **9** with **10**, we can conclude that after displacing of trimethoxy substituent, the potent activity of compounds is maintained. As mentioned in the introduction section, we have designed our new compounds based on trimethoxyphenyl scaffold. In vitro biological evaluation of flexible and rigid analogs derived from 4*H*-1,2,4-triazole revealed that all trimethoxyphenyl derivatives have potent anti-proliferative activity in the range of 0.30–5.0 μM. We have synthesized compounds **9h** and **9i** containing monomethoxyphenyl moiety. The latter compounds showed no significant activity at the concentration of 5.0 μM against tested cancer cell lines. These findings demonstrated the importance of trimethoxyphenyl scaffold in the potential anti-proliferative activity of prototype compounds **9a-g**.

In order to check the selective cytotoxic activity of the designed compounds, we have tested the representative compounds **9a**, **10h** and **10k** against normal cells L929. As seen in Table 3, compound **9a** showed very poor cytotoxic activity (IC_{50} = 487.4 μM) against normal cells. In addition, compounds **10h** and **10k** had no cytotoxic effect on normal cells. Therefore, these potent compounds showed high selectivity and good safety profile in vitro.

Table 3
Cytotoxic activity of selected compound against normal cells L929.

Compound	Structure	(IC_{50}, μM)
9a	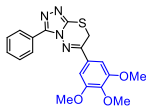	487.4 ± 0.5
10h	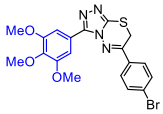	> 500
10k	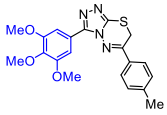	> 500

2.2.2. Tubulin polymerization assay

The most promising anti-proliferative compounds **9a** and **10h** were investigated for their inhibitory activity on tubulin polymerization to confirm that the anti-proliferative activities of these compounds are related to the microtubule targeting. Colchicine was used as a standard tubulin polymerization inhibitor [18,19]. The obtained results for the tubulin polymerization assay of compounds **9a**, **10h** and colchicine are shown in Fig. 3. As seen, these compounds significantly inhibited tubulin polymerization in a dose-dependent manner. The IC_{50} values of compounds **10h** and **9a** were 1.03 and 1.61 μM, respectively, being higher than that of colchicine.

2.2.3. Colchicine-tubulin binding inhibition by compound *10h*

As mentioned in the Introduction section, the trimethoxyphenyl moiety acts as a pharmacophoric group for the tubulin inhibitors such as colchicine (**1**), combretastatin (**2**), and podophyllotoxin (**3**). At the molecular level, these compounds can bind to the colchicine-binding site in tubulin, leading to microtubule depolymerization [3–6]. As we designed our compounds as analogs of the natural tubulin inhibitors containing trimethoxyphenyl moiety, we investigated the possible binding of the promising compound **10h** toward tubulin polymerization in the colchicine-binding site of tubulin. In order to characterize the binding of ligands to tubulin at the colchicine-binding site, the fluorescence of colchicine-tubulin complex has been widely used previously [20–22]. Indeed, the binding affinity of certain ligand to the colchicine-binding site results in the displacement of colchicine molecule by ligand and the reduction of fluorescence intensity. Therefore, we investigated whether compound **10h** can bind to the purified tubulin at the colchicine pocket by determination of changes in the colchicine-tubulin fluorescence. After addition of different concentrations of compound **10h**, changes in the fluorescence intensity were recorded relative to initial intensity, at 430 nm following excitation at 360 nm. As shown in Fig. 4, the addition of compound **10h** to the reaction mixture containing tubulin (0.25 μM) and colchicine (0.1, 0.25, 0.5 or 1 μM) could reduce fluorescence in a concentration-dependent manner (0.1, 0.5, 1, 5, 25 μM). For example, in the presence of compound **10h** (0.5 μM) the relative fluorescence intensity (F/F0) of tubulin-colchicine complex (0.25 μM) was reduced from 1.0 to about 0.5. The significant increment of colchicine-tubulin fluorescence after addition of compound **10h** indicated that this ligand can inhibit the binding of colchicine to tubulin.

2.2.4. Annexin V-FITC flow cytometric analysis of apoptosis

To investigate the potential effects of compounds **10h**, **10k** and **9a** on apoptosis or nonspecific necrosis, the externalized

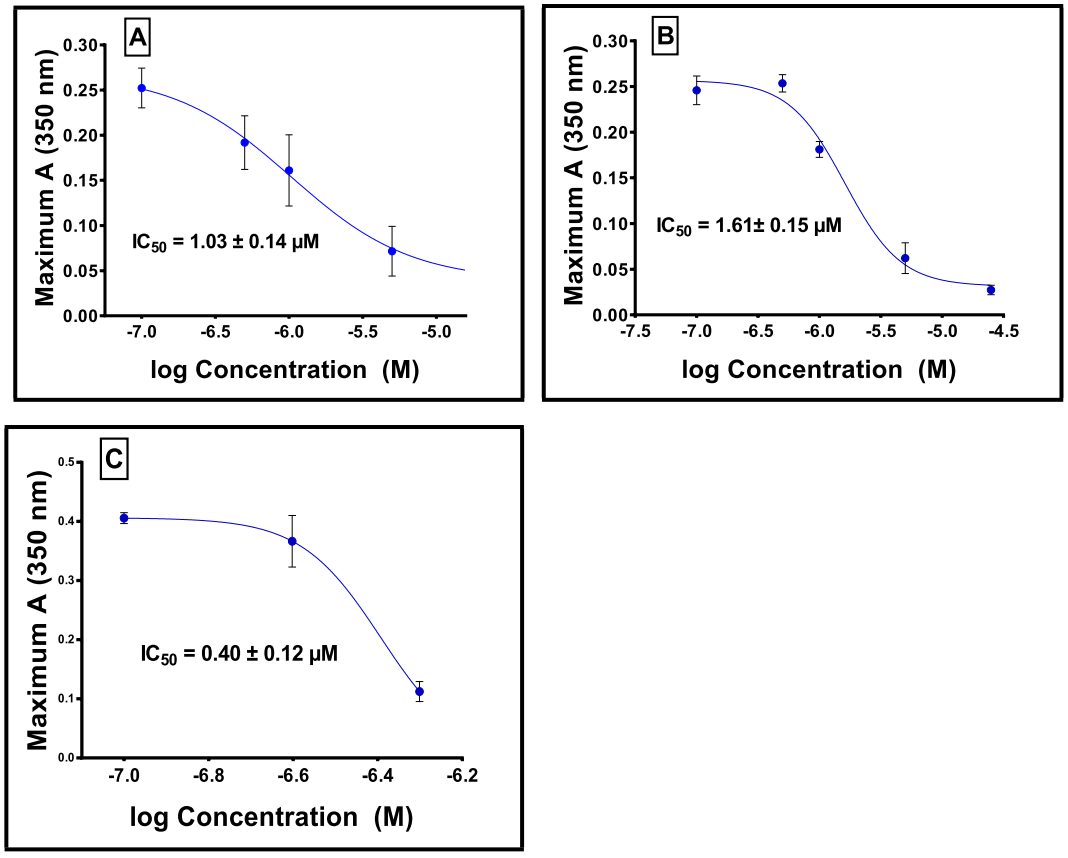

Fig. 3. Effect of compounds **10h** (A), **9a** (B) and colchicine (C) on tubulin polymerization.

phosphatidylserine was detected by Annexin V-FITC/PI dual staining assay [23]. SKOV3 cells were treated with selected compounds at the concentrations of 5 and 10 μM for 48 h, and etoposide was served as the positive control. As illustrated in Fig. 5, after treating with 5 μM of compounds **10h**, **10k** and **9a** apoptosis indices were 18.61, 13.6 and 7.12%, respectively; with 10 μM of compounds **10h**, **10k** and **9a** apoptosis indices increased to 29.27, 16.92 and 9.97%, respectively.

2.3. Molecular docking studies

Molecular modeling was performed in order to confirm the binding of the designed compounds in the colchicine-binding site of tubulin by using AutoDock software (version 4.2). The promising compounds **9a**, **10h** and **10k** were docked into the colchicine-binding site of tubulin using the high resolution crystal structure of the tubulin-colchicine complex, obtained from protein data bank (PDB entry: 4O2B). The obtained binding energies of the compounds **9a**, **10h**, **10k** and colchicine with tubulin were −7.20, −7.82, −7.19, and −8.18 kcal/mol, respectively. As shown in Fig. 6a, the trimethoxyphenyl moiety of **9a** is surrounded by several amino acid residues, such as βLeu252, βAsp251, βLeu255, βAla316, βIle318, βAla317, βCys241, βIle378, βThr240, βVal238, and βLeu242, located in a hydrophobic pocket. Furthermore, the central bicyclic ring of **9a** is in contact with βAla250, βLeu248, βLys254, βMet259, βAsn258, βLys352, βAsn350, βThr314, βVal315, βAla316. The 2D presentation for the binding mode of compound **9a** (Fig. 6b) indicates the formation of a π-σ interaction between the trimethoxyphenyl scaffold and Leu255. Moreover, several π-alkyl and alkyl interactions between the aromatic rings of compound **9a** and amino acid residues Cys241, Ala316, Lys352, Met259, Ala316, Lys254, Leu428 and Ala250 were detected.

The obtained molecular docking results for **10h** demonstrate that the trimethoxyphenyl part is encompassed by βLeu252, βLeu242, βThr239, βLeu255, βVal238, βThr240, Gly237, βIle318, βAla316, βAla317, βAla354 amino acid residues. Notably, a hydrophobic interaction between the bromine atom of ligand and amino acid residue Lys352, a π-σ interaction between the trimethoxyphenyl and Leu255, a π-alkyl bond between trimethoxyphenyl ring and Cys241, Leu248 are involved, as depicted in Fig. 6c and d. In the case of compound **10k**, one hydrogen bond between methoxy group and NH_2-group of Lys254 and one π-sulfur interaction between phenyl group and Met259 were also observed (Fig. 6e and f).

3. Conclusion

We have designed and synthesized flexible and rigid analogs of 4*H*-1,2,4-triazoles (compounds **8** and **9**) bearing trimethoxyphenyl pharmacophoric unit, as potential anticancer agents. The cytotoxicity assay of the compounds against three human cancer cell lines (A549, MCF7, and SKOV3) demonstrated that both flexible and rigid analogs (**8** and **9**, respectively) can potentially inhibit the growth of cancerous cells, with IC_{50} values less than 5.0 μM. Particularly, the flexible analog 5-(3-bromophenyl)-4*H*-1,2,4-triazole (compound **8d**) with IC_{50} value of 0.36 μM, was 6-fold more potent than etoposide (IC_{50} = 2.3 μM) against SKOV3 cells. Also, compound **9d** as direct rigid analog of **8d**, was found to be 4 times more active than etoposide against A549 cell line. In the case of MCF7 cells, the unsubstituted rigid compound **9a** showed the highest activity, displaying IC_{50} value of 0.7 μM. Further displacement of 3,4,5-trimethoxy substituent on the phenyl ring connected to the annulated triazole resulted in compounds **10a-l** with reserving good cytotoxic activity (IC_{50}s < 5.0 μM). Certainly, the 4-bromo and 4-methyl derivatives (**10h** and **10k**) were found to be the best compounds against A549 (IC_{50} = 0.60 μM) and SKOV3 (IC_{50} = 0.30 μM), respectively. Cytotoxicity evaluation of compounds **9a**, **10h** and **10k** against normal cells L929 revealed that these

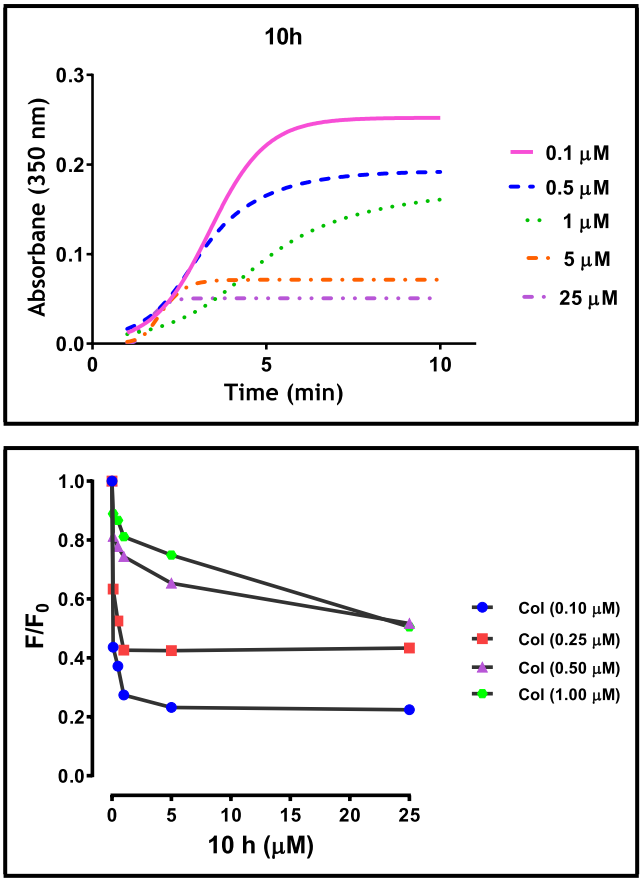

Fig. 4. Characterization of the interaction of compound **10h** with tubulin. (A) Kinetics of the inhibition for compound **10h** at different concentrations against tubulin polymerization; (B) Inhibition of the binding of colchicine to tubulin by compound **10h**. The concentrations of colchicine (Col) are presented in the figure. Compound **10h** were tested at the concentrations of 0, 0.1, 0.5, 1, 5, 25 μM in triplicates.

compounds have high selectivity toward cancer cells. Further evaluation of compounds **9a** and **10h** in tubulin polymerization assay revealed that these compounds effectively inhibit microtubule assembly and disrupt the microtubule polymerization (IC_{50} values = 1.61 and 1.03 μM, respectively). Based on the fluorescence assay, the compound **10h** can inhibit the fluorescence of colchicine-tubulin complex indicating the binding of this compound to the colchicine-binding site. Alternatively, the molecular docking study offers an obvious insight into the binding site of the representative compounds **9a**, **10h** and **10k** with tubulin, and confirms that binding of these compounds to the colchicine-binding site of tubulin causes anti-proliferative activity.

4. Experimental section

4.1. Synthesis

All starting materials and reagents were obtained from Sigma–Aldrich or Merck Company. Commercial solvents were used without any pretreatment. The intermediate compounds **13** and **17** namely 4-amino-5-aryl-4*H*-1,2,4-triazole-3-thiols were synthesized following the reported methods [15,16,24].

4.1.1. General procedure for the preparation of compounds *12a-l*

To a warm stirred suspension of grinded $CuBr_2$ (10 mmol, 2.23 g) in chloroform/ethyl acetate (20 mL, 1:1), appropriate acetophenone **11** (10 mmol) in chloroform (10 mL) was added, and the reaction mixture was vigorously stirred and refluxed for 4 h. After completion of the reaction, the reaction mixture was filtered and the solution was concentrated under reduced pressure to give crude product. Then the oily product was crystallized from hexane-ether to afford pure compound **12**.

4.1.2. General procedure for the preparation of compounds *8a-g*

A mixture of 4-amino-5-(substituted phenyl)-4*H*-[1,2,4]triazole-3-thiol **13** (1 mmol) and K_2CO_3 (152 mg, 1.1 mmol) in dry acetone (4 mL) was stirred at room temperature and then 2-bromo-1-(3,4,5-trimethoxyphenyl)ethan-1-one (**12a**, 289 mg, 1 mmol) was added and the stirring was continued for 1–5 h (monitored by TLC). After completion of the reaction, the precipitated solids were collected by filtration, washed with water and dried to give pure compounds **8a-g**.

Compound 8a: Yield: 72%; m.p: 201–203 °C; ^{1}H NMR (400 MHz, $CDCl_3$): δ 3.95 (s, 6H, OMe), 3.96 (s, 3H, OMe), 4.01 (s, 2H, CH_2), 5.30 (s, 2H, NH_2), 7.16 (s, 2H, H-2′ and H-6′), 7.49–7.55 (m, 3H, H-3, H-4 and H-5), 8.13–8.17 (m, 2H, H-2 and H-6). MS (*m/z*, %) 401 (M^+ +1, < 1), 400 (M^+, < 1), 371 (1), 316 (13), 210 (18), 195 (27), 167 (12), 149 (58), 135 (10), 111 (14), 85 (27), 71 (51), 57 (100). Anal. Calcd for $C_{19}H_{20}N_4O_4S$: C, 56.99; H, 5.03; N, 13.99. Found: C, 57.21; H, 5.09; N, 14.22.

Compound 8b: Yield: 72%; m.p: 260–262 °C; ^{1}H NMR (250 MHz, $CDCl_3$): δ 2.44 (s, 3H, Me), 3.95 (s, 6H, OMe), 3.96 (s, 3H, OMe), 4.25 (s, 2H, CH_2), 7.16 (s, 2H, H-2′ and H-6′), 7.35 (m, 2H, H-3 and H-5), 8.15 (m, 2H, H-2 and H-6). MS (*m/z*, %) 414 (M^+, < 1), 352 (100), 336 (58), 190 (14), 163 (32), 132 (19), 103 (64), 77 (23), 51 (14). Anal. Calcd for $C_{20}H_{22}N_4O_4S$: C, 57.96; H, 5.35; N, 13.52. Found: C, 58.19; H, 5.37; N, 13.40.

Compound 8c: Yield: 68%; m.p: 247–249 °C; ^{1}H NMR (400 MHz, DMSO-d_6): δ 3.77 (s, 3H, OMe), 3.88 (s, 6H, OMe), 4.45 (s, 2H, CH_2), 6.95 (d, 2H, *J* = 8.8 Hz, H-3 and H-5), 7.35 (s, 2H, H-2′ and H-6′), 7.90 (d, 2H, *J* = 8.8 Hz, H-2 and H-6). MS (*m/z*, %) 416 (M^+, < 1), 281 (10), 207 (100), 190 (11), 162 (6), 132 (15), 119 (8), 103 (10), 96 (11), 63 (23), 58 (18). Anal. Calcd for $C_{19}H_{20}N_4O_5S$: C, 54.80; H, 4.84; N, 13.45. Found: C, 55.88; H, 4.69; N, 13.53.

Compound 8d: Yield: 78%; m.p: 228–230 °C; ^{1}H NMR (400 MHz, DMSO-d_6): δ 3.78 (s, 3H, OMe), 3.91 (s, 6H, OMe), 4.49 (s, 2H, CH_2), 7.38 (s, 1H, H-2′ and H-6′), 7.58 (t, 1H, *J* = 8.0 Hz, H-5), 7.79 (d, 1H, *J* = 8.0 Hz, H-4), 8.10 (d, 1H, *J* = 8.0 Hz, H-6), 8.32 (s, 1H, H-2). MS (*m/z*, %) 478 (M^+, < 1), 310 (35), 302 (34), 281 (15), 207 (74), 195 (42), 181 (18), 149 (10), 133 (16), 119 (11), 102 (32), 83 (10), 75 (16), 67 (27), 60 (100), 51 (11). Anal. Calcd for $C_{19}H_{19}BrN_4O_4S$: C, 47.61; H, 4.00; N, 11.69. Found: C, 47.60; H, 4.11; N, 11.67.

Compound 8e: Yield: 73%; m.p: 221–223 °C; ^{1}H NMR (400 MHz, DMSO-d_6): δ 3.78 (s, 3H, OMe), 3.89 (s, 6H, OMe), 4.49 (s, 2H, CH_2), 5.18 (s, 2H, NH_2), 7.14 (d, 2H, *J* = 8.8 Hz, H-3 and H-5), 7.39 (s, 2H, H-2′ and H-6′), 7.89 (d, 2H, *J* = 8.8 Hz, H-2 and H-6). ^{13}C NMR (100 MHz, DMSO-d_6): δ 191.28, 166.04, 163.02, 162.37, 153.29, 130.02, 129.79, 128.52, 115.97, 114.51, 106.06, 61.06, 56.43, 55.46, 41.12. MS (*m/z*, %) 430 (M^+, < 1), 416 (6), 281 (4), 222 (15), 207 (21), 195 (100), 175 (6), 151 (5), 133 (37), 119 (4), 103 (5), 91 (25), 77 (11), 64 (6), 51 (4). Anal. Calcd for $C_{20}H_{22}N_4O_5S$: C, 55.80; H, 5.15; N, 13.02. Found: C, 56.02; H, 5.16; N, 12.87.

Compound 8f: Yield: 65%; m.p: 236–238 °C; ^{1}H NMR (400 MHz, DMSO-d_6): δ 3.77 (s, 3H, OMe), 3.89 (s, 6H, OMe), 4.49 (s, 2H, CH_2), 7.35 (s, 2H, H-2′ and H-6′), 7.70 (d, 2H, *J* = 8.4 Hz, H-3 and H-5), 8.11 (d, 2H, *J* = 8.8 Hz, H-2 and H-6). MS (*m/z*, %) 434 (M^+, < 1), 416 (10), 401 (8), 281 (17), 225 (7), 207 (75), 195 (35), 178 (7), 151 (5), 137 (17), 125 (10), 113 (12), 97 (24), 85 (62), 71 (75), 57 (100). Anal. Calcd for $C_{19}H_{19}ClN_4O_4S$: C, 52.47; H, 4.40; N, 12.88. Found: C, 52.53; H, 4.49; N, 13.03.

Compound 8g: Yield: 62%; m.p: 240–242 °C; ^{1}H NMR (400 MHz, DMSO-d_6): δ 3.74 (s, 3H, OMe), 3.82 (s, 6H, OMe), 4.49 (s, 2H, CH_2), 5.21 (s, 2H, NH_2), 7.21 (s, 2H, H-2′ and H-6′), 7.69 (d, 1H, H-5), 7.74 (s, 1H, H-3), 7.93 (d, 1H, H-6). MS (*m/z*, %) 468 (M^+, < 1), 281 (5), 230 (12), 207 (35), 195 (100), 185 (5), 173 (13), 149 (13), 105 (71), 95 (9),

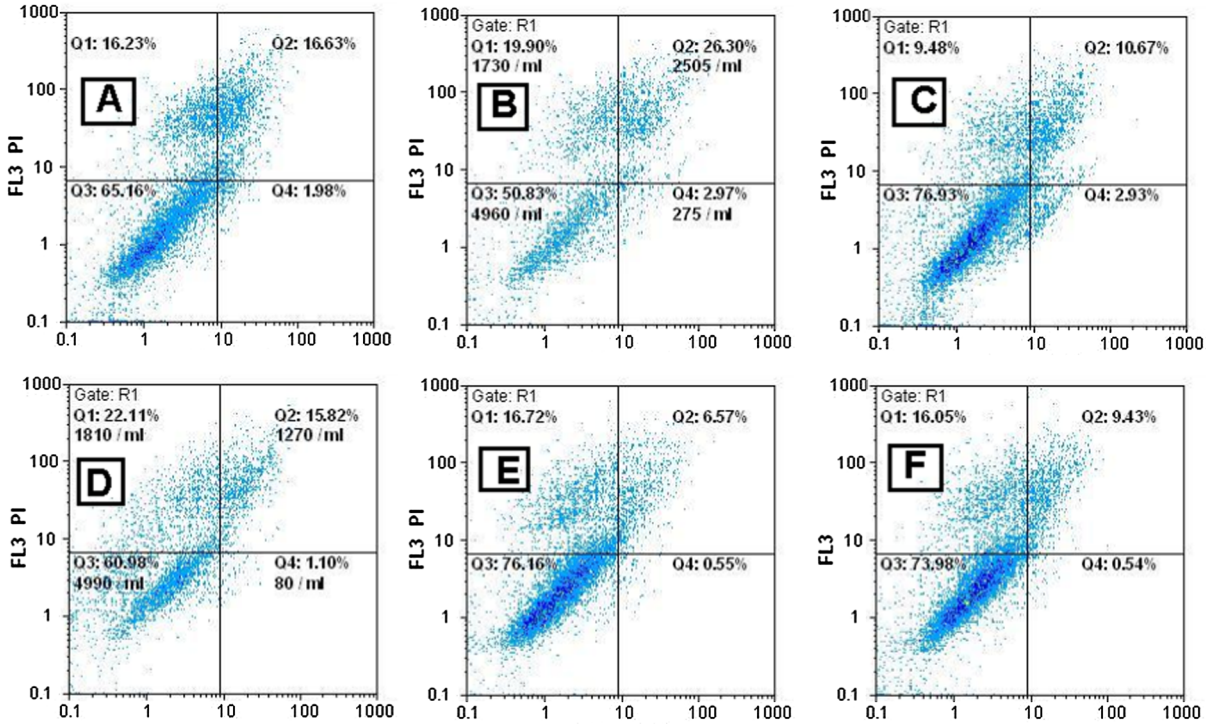

Fig. 5. Flow cytometric analysis in SKOV3 cell line after treatment with compounds **10h**, **10k** and **9a** at 5 and 10 μM concentrations for 48 h; A: **10h** (5 μM), B: **10h** (10 μM), C: **10k** (5 μM), D: **10k** (10 μM), E: **9a** (5 μM), F: **9a** (10 μM).

85 (12), 77 (34), 57 (13). Anal. Calcd for $C_{19}H_{18}Cl_2N_4O_4S$: C, 48.62; H, 3.87; N, 11.94. Found: C, 48.56; H, 3.79; N, 11.91.

*4.1.3. General procedure for the preparation of compounds **9a-i***

A solution of 4-amino-5-(substituted phenyl)-4*H*-[1,2,4]triazole-3-thiol **13** (1 mmol) and desired phenacyl bromide (**12a** or **12b**, 1.2 mmol) in absolute ethanol (7 mL) was refluxed for 1–5 h. After cooling to room temperature, the reaction mixture was left in refrigerator overnight. The precipitated solid was separated and washed with cool ethanol. The crude product was recrystallized from ethanol to give pure compounds **9a-i**.

Compound 9a: Yield: 80%; m.p: 213–215 °C; ^{1}H NMR (400 MHz, DMSO-d_6): δ 3.76 (s, 3H, OMe), 3.86 (s, 6H, OMe), 4.47 (s, 2H, CH_2), 7.34 (s, 2H, H-2′ and H-6′), 7.54–7.63 (m, 3H, H-3, H-4 and H-5), 8.05 (dd, 2H, J = 8.0 and 1.6 Hz, H-2 and H-6). MS (*m/z*, %) 382 (M^+ < 1), 316 (5), 266 (19), 207 (45), 191 (9), 150 (26), 140 (9), 129 (16), 119 (11), 109 (8), 96 (16), 82 (100), 69 (22), 57 (44). Anal. Calcd for $C_{19}H_{18}N_4O_3S$: C, 59.67; H, 4.74; N, 14.65. Found: C, 59.91; H, 4.75; N, 14.77.

Compound 9b: Yield: 75%; m.p: 257–259 °C; ^{1}H NMR (400 MHz, DMSO-d_6): δ 2.39 (s, 3H, Me), 3.76 (s, 3H, OMe), 3.87 (s, 6H, OMe), 4.45 (s, 2H, CH_2), 7.33 (s, 2H, H-2′ and H-6′), 7.39 (d, 2H, J = 8.0 Hz, H-3 and H-5), 7.96 (d, 2H, J = 8.4 Hz, H-2 and H-6). ^{13}C NMR (100 MHz, DMSO-d_6): δ 156.10, 153.57, 151.87, 142.69, 141.22, 140.57, 129.74, 129.07, 128.22, 123.66, 105.68, 60.69, 56.60, 23.12, 21.48. MS (*m/z*, %) 396 (M^+, 100), 381 (85), 322 (5), 236 (3), 207 (5), 193 (13), 178 (5), 163 (5), 149 (5), 133 (8), 117 (36), 103 (5), 90 (11), 77 (7), 58 (9). Anal. Calcd for $C_{20}H_{20}N_4O_3S$: C, 60.59; H, 5.08; N, 14.13. Found: C, 60.58; H, 4.71; N, 14.00.

Compound 9c: Yield: 63%; m.p: 295–297 °C; ^{1}H NMR (400 MHz, DMSO-d_6): δ 3.76 (s, 3H, OMe), 3.87 (s, 6H, OMe), 4.44 (s, 2H, CH_2), 6.94 (d, 2H, J = 8.4 Hz, H-3 and H-5), 7.33 (s, 2H, H-2′ and H-6′), 7.89 (d, 2H, J = 8.4 Hz, H-2 and H-6), 10.05 (brs, 1H, OH). MS (*m/z*, %) 398 (M^+, 5), 380 (17), 365 (6), 239 (8), 221 (46), 207 (100), 188 (12), 174 (19), 147 (14), 134 (24), 120 (74), 105 (8), 88 (19), 64 (24). Anal. Calcd for $C_{19}H_{18}N_4O_4S$: C, 57.28; H, 4.55; N, 14.06. Found: C, 57.41; H, 4.58; N, 13.85.

Compound 9d: Yield: 80%; m.p: 290–292 °C; ^{1}H NMR (400 MHz, DMSO-d_6): δ 3.76 (s, 3H, OMe), 3.89 (s, 6H, OMe), 4.49 (s, 2H, CH_2), 7.36 (s, 2H, H-2′ and H-6′), 7.57 (t, 1H, J = 8.0 Hz, H-5), 7.76–7.80 (m, 1H, H-6), 8.09 (dt, 1H, J = 8.0 and 1.6 Hz, H-4), 8.31 (dd, 1H, J = 2.0 and 1.6 Hz, H-2). MS (*m/z*, %) 462 (M + 2, 100), 460 (M^+, 99), 447 (55), 445 (54), 430 (5), 366 (18), 351 (7), 271 (36), 269 (35), 255 (23), 253 (23), 236 (11), 207 (17), 193 (30), 181 (35), 163 (12), 149 (12), 135 (13), 120 (22), 102 (55), 75 (18), 58 (12). Anal. Calcd for $C_{19}H_{17}BrN_4O_3S$: C, 49.47; H, 3.71; N, 12.14. Found: C, 49.36; H, 3.80; N, 12.18.

Compound 9e: Yield: 63%; m.p: 286–288 °C; ^{1}H NMR (400 MHz, DMSO-d_6): δ 3.76 (s, 3H, OMe), 3.84 (s, 3H, OMe), 3.87 (s, 6H, OMe), 4.45 (s, 2H, CH_2), 7.14 (d, 2H, J = 8.8 Hz, H-3 and H-5), 7.33 (s, 2H, H-2′ and H-6′), 8.00 (d, 2H, J = 8.8 Hz, H-2 and H-6). ^{13}C NMR (100 MHz, DMSO-d_6): δ 161.22, 155.98, 153.57, 151.74, 142.31, 141.20, 129.91, 129.12, 118.82, 114.64, 105.65, 56.62, 55.86, 23.12. MS (*m/z*, %) 412 (M^+, 5), 398 (47), 383 (40), 366 (100), 351 (45), 323 (7), 292 (5), 270 (7), 251 (6), 236 (9), 221 (12), 207 (49), 193 (56), 178 (34), 163 (23), 149 (33), 135 (29), 119 (78), 102 (60), 91 (40), 76 (27), 63 (29). Anal. Calcd for $C_{20}H_{20}N_4O_4S$: C, 58.24; H, 4.89; N, 13.58. Found: C, 58.27; H, 5.03; N, 13.62.

Compound 9f: Yield: 88%; m.p: 277–279 °C; ^{1}H NMR (400 MHz, DMSO-d_6): δ 3.76 (s, 3H, OMe), 3.87 (s, 6H, OMe), 4.47 (s, 2H, CH_2), 7.33 (s, 2H, H-2′ and H-6′), 7.68 (d, 2H, J = 8.4 Hz, H-3 and H-5), 8.09 (d, 2H, J = 8.8 Hz, H-2 and H-6). ^{13}C NMR (100 MHz, DMSO-d_6): δ 156.42, 155.21, 153.58, 150.92, 143.24, 135.52, 129.93, 129.39, 128.90, 125.28, 105.73, 60.40, 56.60, 23.17. MS (*m/z*, %) 418 (M + 2, 8), 416 (M^+, 21), 401 (16), 336 (100), 321 (25), 203 (10), 175 (11), 160 (5), 147 (28), 133 (38), 117 (46), 103 (11), 90 (22), 77 (15), 58 (16). Anal. Calcd for $C_{19}H_{17}ClN_4O_3S$: C, 54.74; H, 4.11; N, 13.44. Found: C, 54.85; H, 4.33; N, 13.28.

Compound 9g: Yield: 57%; m.p: 272–274 °C; ^{1}H NMR (400 MHz, DMSO-d_6): δ 3.72 (s, 3H, OMe), 3.80 (s, 6H, OMe), 4.47 (s, 2H, CH_2), 7.20 (s, 2H, H-2′ and H-6′), 7.67 (dd, 1H, J = 8.4 and 2.0 Hz, H-5), 7.73 (d, 1H, J = 8.4 Hz, H-6), 7.91 (d, 1H, J = 2.0 Hz, H-3). ^{13}C NMR

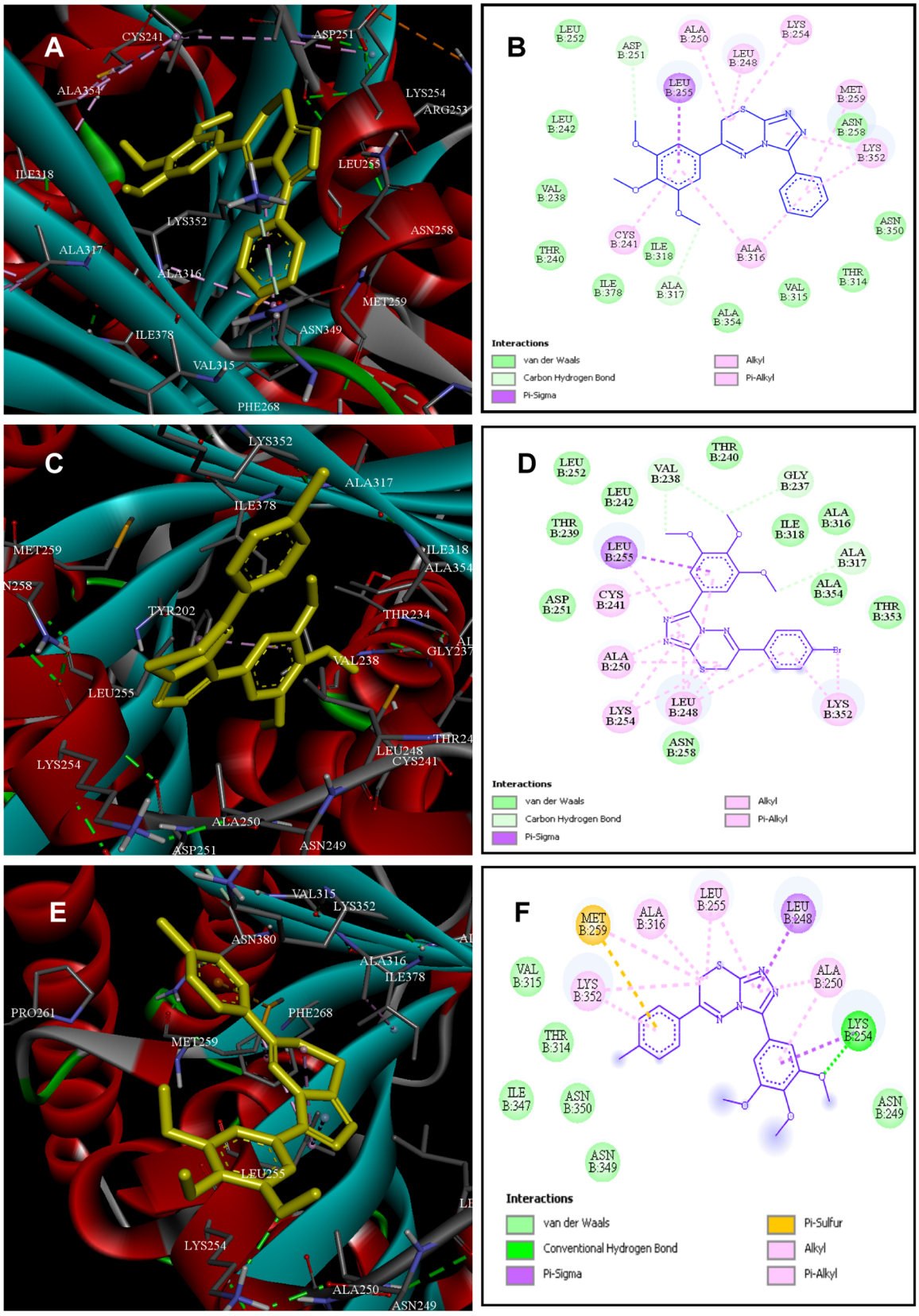

Fig. 6. Binding modes of compounds **9a** (A, B), **10h** (C, D) and **10k** (E, F) with tubulin (PDB ID: 4O2B).

(100 MHz, DMSO-d_6): δ 156.16, 153.49, 150.09, 142.56, 141.32, 136.67, 134.67, 134.38, 130.11, 128.97, 128.06, 124.79, 105.77, 60.67, 56.51, 23.80. MS (*m/z*, %) 450 (M^+, 24), 435 (15), 398 (44), 383 (35), 366 (31), 351 (11), 281 (11), 262 (8), 236 (8), 221 (17), 207 (100), 193 (46), 178 (26), 163 (24), 149 (42), 135 (35), 119 (71), 91 (35), 77 (35), 64 (48), 51 (20). Anal. Calcd for $C_{19}H_{16}Cl_2N_4O_3S$: C, 50.56; H, 3.57; N, 12.41. Found: C, 50.87; H, 3.33; N, 12.45.

Compound 9h: Yield: 72%; m.p: 245–247 °C; ^{1}H NMR (400 MHz,

DMSO-d_6): δ 3.86 (s, 3H, OMe), 4.42 (s, 2H, CH_2), 7.13 (d, 2H, J = 8.8 Hz, H-3′ and H-5′), 7.53–7.62 (m, 3H, H-3, H-4 and H-5), 7.99 (d, 2H, J = 8.8 Hz, H-2′ and H-6′), 8.02 (dd, 2H, J = 8.0 and 2.0 Hz, H-2 and H-6). ^{13}C NMR (100 MHz, DMSO-d_6): δ 162.94, 156.78, 151.62, 143.71, 131.15, 130.09, 129.32, 128.60, 125.70, 125.65, 115.11, 56.09, 23.10. MS (*m/z*, %) 322 (M^+, 100), 307 (31), 147 (24), 133 (30), 118 (5), 103 (35), 77 (12), 58 (7). Anal. Calcd for $C_{17}H_{14}N_4OS$: C, 63.34; H, 4.38; N, 17.38. Found: C, 63.68; H, 4.29; N, 17.40.

Compound 9i: Yield: 66%; m.p: 264–266 °C; ^{1}H NMR (400 MHz, DMSO-d_6): δ 2.40 (s, 3H, Me), 3.85 (s, 3H, OMe), 4.42 (s, 2H, CH_2), 7.13 (d, 2H, J = 8.8 Hz, H-3′ and H-5′), 7.39 (d, 2H, J = 8.0 Hz, H-3 and H-5), 7.90 (d, 2H, J = 8.4 Hz, H-2 and H-6), 7.99 (d, 2H, J = 8.8 Hz, H-2′ and H-6′). MS (*m/z*, %) 336 (M^+, 40), 318 (100), 306 (20), 265 (39), 237 (14), 205 (21), 161 (10), 150 (44), 133 (52), 117 (50), 103 (14), 89 (31), 77 (25), 63 (20), 51 (12). Anal. Calcd for $C_{18}H_{16}N_4OS$: C, 64.27; H, 4.79; N, 16.65. Found: C, 64.01; H, 4.81; N, 16.58.

*4.1.4. General procedure for the preparation of compounds **10a-l***

A solution of compound **17** (282 mg, 1 mmol) and proper phenacyl bromide **12a-l** (1.2 mmol) in absolute ethanol (7 mL) was refluxed for 1–5 h. After cooling to room temperature, the reaction mixture was left in refrigerator overnight. The precipitated solid was separated and washed with cool ethanol. The crude product was recrystallized from ethanol to give corresponding pure compounds **10**.

Compound 10a: Yield: 87%; m.p: 198–200 °C; ^{1}H NMR (250 MHz, $CDCl_3$): δ 3.92 (s, 6H, OMe), 3.94 (s, 3H, OMe), 4.14 (s, 2H, CH_2), 7.53 (s, 2H, H-2 and H-6), 7.54–7.75 (m, 3H, H-3′, H-4′ and H-5′), 7.96 (d, 2H, J = 7.0 Hz, H-2′ and H-6′). ^{13}C NMR (100 MHz, DMSO-d_6): δ 156.29, 153.40, 151.61, 142.85, 139.59, 133.89, 132.52, 129.64, 127.88, 121.71, 105.74, 60.67, 56.41, 23.03. MS (*m/z*, %) 382 (M^+, 100), 364 (27), 264 (4), 193 (47), 178 (25), 163 (3), 135 (13), 103 (17), 77 (17). Anal. Calcd for $C_{19}H_{18}N_4O_3S$: C, 59.67; H, 4.74; N, 14.65. Found: C, 59.50; H, 5.01; N, 14.65.

Compound 10b: Yield: 76%; m.p: 230–232 °C; ^{1}H NMR (400 MHz, DMSO-d_6): δ 3.82 (s, 3H, OMe), 3.92 (s, 9H, OMe), 4.49 (s, 2H, CH_2), 7.22 (d, 2H, J = 8.8 Hz, H-3′ and H-5′), 7.48 (s, 2H, H-2 and H-6), 8.11 (d, 2H, J = 8.8 Hz, H-2′ and H-6′). ^{13}C NMR (100 MHz, DMSO-d_6): δ 162.82, 155.83, 153.38, 151.40, 142.81, 139.53, 129.75, 125.90, 121.84, 115.07, 105.68, 60.64, 56.45, 56.03, 22.80. MS (*m/z*, %) 412 (M^+, 100), 397 (21), 382 (29), 264 (8), 193 (57), 177 (30), 143 (14), 133 (33), 103 (10), 77 (15), 51 (3). Anal. Calcd for $C_{20}H_{20}N_4O_4S$: C, 58.24; H, 4.89; N, 13.58. Found: C, 58.27; H, 5.00; N, 13.37.

Compound 10c: Yield: 84%; m.p: 238–240 °C; ^{1}H NMR (400 MHz, DMSO-d_6): δ 3.84 (s, 3H, OMe), 3.91 (s, 3H, OMe), 3.94 (s, 6H, OMe), 3.95 (s, 3H, OMe), 4.53 (s, 2H, CH_2), 7.26 (d, 1H, J = 8.4 Hz, H-5′), 7.49 (s, 2H, H-2 and H-6), 7.69 (d, 1H, J = 2.0 Hz, H-2′), 7.77 (dd, 1H, J = 8.4 and 2.0 Hz, H-6′). MS (*m/z*, %) 442 (M^+, 26), 424 (100), 410 (57), 281 (69), 267 (83), 252 (42), 224 (15), 209 (16), 193 (30), 178 (26), 163 (26), 135 (14), 120 (16), 104 (7), 79 (9), 64 (16). Anal. Calcd for $C_{21}H_{22}N_4O_5S$: C, 57.00; H, 5.01; N, 12.66. Found: C, 57.01; H, 4.89; N, 12.70.

Compound 10d: Yield: 72%; m.p: 210–212 °C; ^{1}H NMR (400 MHz, DMSO-d_6): δ 3.88 (s, 3H, OMe), 3.89 (s, 3H, OMe), 3.97 (s, 6H, OMe), 3.98 (s, 6H, OMe), 4.59 (s, 2H, CH_2), 7.48 (s, 2H, H-2′ and H-6′), 7.52 (s, 2H, H-2 and H-6). ^{13}C NMR (100 MHz, DMSO-d_6): δ 156.43, 153.62, 153.42, 151.55, 143.22, 141.46, 139.87, 129.09, 121.62, 106.19, 105.88, 60.73, 56.64, 23.38. MS (*m/z*, %) 472 (M^+, 6), 454 (38), 439 (15), 281 (100), 267 (82), 252 (44), 238 (20), 224 (20), 209 (15), 193 (38), 178 (32), 164 (8), 150 (17), 135 (17), 120 (16), 93 (6), 79 (6), 64 (16). Anal. Calcd for $C_{22}H_{24}N_4O_6S$: C, 55.92; H, 5.12; N, 11.86. Found: C, 55.61; H, 5.06; N, 12.05.

Compound 10e: Yield: 68%; m.p: 204–206 °C; ^{1}H NMR (400 MHz, DMSO-d_6): δ 3.84 (s, 3H, OMe), 3.93 (s, 6H, OMe), 4.54 (s, 2H, CH_2), 7.47 (s, 2H, H-2 and H-6), 7.55 (t, 2H, J = 8.8 Hz, H-3′ and H-5′), 8.22 (dd, 2H, J = 8.4 and 5.6 Hz, H-2′ and H-6′). MS (*m/z*, %) 400 (M^+, 100), 385 (30), 368 (27), 193 (54), 178 (33), 150 (12), 135 (25), 120 (18), 95 (12), 75 (6). Anal. Calcd for $C_{19}H_{17}FN_4O_3S$: C, 56.99; H, 4.28; N, 13.99. Found: C, 57.02; H, 4.13; N, 13.92.

Compound 10f: Yield: 65%; m.p: 215–217 °C; ^{1}H NMR (400 MHz, DMSO-d_6): δ 3.73 (s, 3H, OMe), 3.82 (s, 6H, OMe), 4.36 (s, 2H, CH_2), 7.30–7.35 (m, 1H, H-3′), 7.36 (s, 2H, H-2 and H-6), 7.52–7.59 (m, 1H, H-5′), 7.94–8.00 (m, 1H, H-6′). MS (*m/z*, %) 418 (M^+, 100), 403 (36), 386 (26), 371 (9), 267 (9), 252 (5), 193 (55), 178 (35), 163 (5), 139 (20), 120 (14), 64 (5). Anal. Calcd for $C_{19}H_{16}F_2N_4O_3S$: C, 54.54; H, 3.85; N, 13.39. Found: C, 54.75; H, 3.86; N, 13.43.

Compound 10g: Yield: 82%; m.p: 216–218 °C; ^{1}H NMR (400 MHz, DMSO-d_6): δ 3.86 (s, 3H, OMe), 3.94 (s, 6H, OMe), 4.55 (s, 2H, CH_2), 7.47 (s, 2H, H-2 and H-6), 7.79 (d, 2H, J = 8.8 Hz, H-3′ and H-5′), 8.18 (d, 2H, J = 8.8 Hz, H-2′ and H-6′). ^{13}C NMR (100 MHz, DMSO-d_6): δ 155.25, 153.40, 151.64, 142.73, 139.62, 137.33, 132.73, 129.73, 129.64, 121.61, 105.75, 60.63, 56.41, 22.92. MS (*m/z*, %) 416 (M^+, 100), 401 (29), 281 (5), 264 (5), 193 (77), 178 (44), 150 (20), 135 (22), 120 (20), 102 (13), 75 (12), 58 (5). Anal. Calcd for $C_{19}H_{17}ClN_4O_3S$: C, 54.74; H, 4.11; N, 13.44. Found: C, 54.75; H, 3.96; N, 13.33.

Compound 10h: Yield: 92%, m.p: 241–243 °C; ^{1}H NMR (400 MHz, DMSO-d_6): δ 3.76 (s, 3H, OMe), 3.85 (s, 6H, OMe), 4.45 (s, 2H, CH_2), 7.38 (s, 2H, H-2 and H-6), 7.83 (d, 2H, J = 8.8 Hz, H-3′ and H-5′), 8.00 (d, 2H, J = 8.8 Hz, H-2′ and H-6′). ^{13}C NMR (100 MHz, DMSO-d_6): δ 155.50, 153.40, 151.61, 142.84, 139.66, 133.06, 132.68, 129.81, 126.34, 121.49, 105.79, 60.64, 56.44, 22.90. MS (*m/z*, %) 462 (M + 2, 69), 460 (M^+, 68), 447 (15), 416 (19), 401 (7), 281 (11), 264 (7), 208 (14), 193 (93), 178 (53), 150 (26), 135 (28), 120 (26), 102 (30), 80 (100), 64 (12). Anal. Calcd for $C_{19}H_{17}BrN_4O_3S$: C, 49.47; H, 3.71; N, 12.14. Found: C, 49.45; H, 4.01; N, 12.37.

Compound 10i: Yield: 72%; m.p: 263–265 °C; ^{1}H NMR (400 MHz, DMSO-d_6): δ 3.85 (s, 3H, OMe), 3.96 (s, 6H, OMe), 4.48 (s, 2H, CH_2), 7.04 (d, 2H, J = 8.8 Hz, H-3′ and H-5′) 7.51 (s, 2H, H-2 and H-6), 8.04 (d, 2H, J = 8.8 Hz, H-2′ and H-6′). ^{13}C NMR (100 MHz, DMSO-d_6): δ 161.81, 156.47, 153.37, 151.07, 143.21, 139.73, 129.99, 124.07, 121.22, 116.46, 105.81, 60.66, 56.39, 22.75. MS (*m/z*, %) 398 (M^+, 15), 380 (14), 296 (13), 281 (100), 266 (47), 238 (16), 223 (14), 208 (16), 193 (54), 178 (38), 150 (23), 135 (38), 120 (58), 104 (9), 80 (18), 64 (20). Anal. Calcd for $C_{19}H_{18}N_4O_4S$: C, 57.28; H, 4.55; N, 14.06. Found: C, 57.50; H, 4.56; N, 14.02.

Compound 10j: Yield: 77%; m.p: 255–257 °C; ^{1}H NMR (400 MHz, DMSO-d_6): δ 3.85 (s, 3H, OMe), 3.95 (s, 6H, OMe), 4.44 (s, 2H, CH_2), 6.99 (d, 1H, J = 8.4 Hz, H-5′) 7.48 (s, 2H, H-2 and H-6), 7.49 (dd, 1H, J = 8.4 and 2.4 Hz, H-6′), 7.65 (d, 1H, J = 2.4 Hz, H-2′). MS (*m/z*, %) 414 (M^+, 19), 398 (19), 295 (15), 281 (100), 267 (46), 255 (45), 238 (19), 223 (15), 207 (93), 196 (87), 178 (59), 150 (34), 135 (45), 120 (40), 93 (21), 77 (22), 58 (47). Anal. Calcd for $C_{19}H_{18}N_4O_5S$: C, 55.06; H, 4.38; N, 13.52. Found: C, 54.98; H, 4.39; N, 13.86.

Compound 10k: Yield: 78%; m.p: 230–232 °C; ^{1}H NMR (400 MHz, DMSO-d_6): δ 2.39 (s, 3H, Me), 3.76 (s, 3H, OMe), 4.36 (s, 6H, OMe), 4.44 (s, 2H, CH_2), 7.40 (d, 4H, J = 8.0 Hz, H-3′ and H-5′), 7.41 (s, 2H, H-2 and H-6), 7.97 (d, 2H, J = 8.0 Hz, H-2′ and H-6′). ^{13}C NMR (100 MHz, DMSO-d_6): δ 156.45, 153.38, 151.5, 142.95, 142.90, 139.70, 130.93, 130.22, 127.88, 121.40, 105.80, 60.65, 56.45, 22.91, 21.53. MS (*m/z*, %) 396 (M^+, 19), 381 (21), 281 (29), 266 (10), 207 (7), 193 (79), 178 (40), 150 (19), 135 (21), 117 (21), 91 (20), 64 (20). Anal. Calcd for $C_{20}H_{20}N_4O_3S$: C, 60.59; H, 5.08; N, 14.13. Found: C, 60.83; H, 5.36; N, 14.12.

Compound 10l: Yield: 83%; m.p: 248–250 °C; ^{1}H NMR (400 MHz, DMSO-d_6): δ 3.78 (s, 3H, OMe), 3.89 (s, 6H, OMe), 4.52 (s, 2H, CH_2), 7.44 (s, 2H, H-2 and H-6), 7.46 (t, 1H, J = 7.6 Hz, H-4″), 7.54 (t, 2H, J = 7.2 Hz, H-3″ and H-5″), 7.80 (d, 2H, J = 7.2 Hz, H-2″ and H-6″), 7.94 (d, 2H, J = 8.8 Hz, H-3′ and H-5′), 8.18 (d, 2H, J = 8.4 Hz, H-2′

and H-6′). MS (*m/z*, %) 458 (M^+, 3), 440 (100), 425 (22), 367 (4), 282 (11), 281 (38), 267 (72), 252 (22), 224 (15), 209 (8), 194 (18), 179 (67), 152 (33), 135 (8), 120 (11), 96 (8), 79 (5), 64 (33). Anal. Calcd for $C_{25}H_{22}N_4O_3S$: C, 65.49; H, 4.84; N, 12.22. Found: C, 65.21, H, 4.96, N, 12.16.

4.2. Biological tests

4.2.1. MTT assay

The in vitro anti-proliferative activities of synthesized compounds **8–10** in comparison with etoposide (as standard drug) were evaluated against three human cancer cell lines including A549, MCF7, and SKOV3. Furthermore, the selected compounds **9a**, **10h**, and **10k** were tested against normal mouse fibroblast cells L929. Approximately 10^4 cells were seeded in 96-well plate in RPMI supplemented with 10% FBS and incubated for 24 h at 37 °C in CO_2 incubator. Then, cells were treated with 10 μL of compounds, which were diluted in RPMI to appropriate concentrations. After 48 h of incubation, 10 μL of MTT (3-(4,5-dimethylthiazol-2-yl)-2,5-diphenyltetrazolium bromide) (5 mg/mL) was added to each well, followed by 4 h additional incubation. Subsequently after carefully removal of supernatant, the formazan crystals were dissolved in DMSO (200 μL). Finally, the absorbance was recorded at 490 nm wavelength using microplate reader (Bioteck) [17]. IC_{50} values were calculated with GraphPad Prism software version 6.0.

4.2.2. Tubulin polymerization assay

Tubulin was purified from sheep brain according to the method of Williams and Lee [25]. In order to evaluate the inhibitory effect of compounds **9a** and **10h** on tubulin polymerization in comparison to colchicine, tubulin was incubated in the presence and absence of compounds **9a** and **10h** (at the concentrations of 0.1, 0.5, 1, 5, or 25 μM) and colchicine (0, 0.1, 0.25, or 0.5 μM) for 15 min on ice. Then, tubulin polymerization was induced by adding GTP to a final concentration of 1 mM at 37 °C. Tubulin assembly was determined turbidimertically at 350 nm [26]. To determine the concentration that inhibited tubulin polymerization by 50% (IC_{50}) the area under the curve (AUC) was used. The AUC of the untreated controls were set to 100% polymerization. IC_{50} values were calculated with GraphPad Prism software version 6.0.

4.2.3. Fluorescence assay for colchicine-tubulin binding

To examine the inhibition of the binding of colchicine to tubulin by the designed compounds, the most potent tubulin inhibitor **10h** was tested using fluorescence technique as reported previously [27,28]. Briefly, tubulin 0.25 μM was incubated with increasing concentrations of colchicine (0.1, 0.25, 0.5 or 1 μM) for 1 h at 37 °C. Compound **10h** was added to the tubulin-colchicine complexes to a final concentration of 0.1, 0.5, 1, 5, 25 μM. Fluorescence emission spectra were recorder at 430 nm following excitation at 360 nm using Cytation 3, multi-mode imaging and plate Reader (BioTek, USA), (n = 3). Fluorescent data was corrected by subtracting the background fluorescence intensity for compound **10h** at given concentrations. "F_0" and "F" are the fluorescence intensity (a.u) of the [tubulin + colchicine] and [tubulin + colchicine + compound **10h**] mixtures, respectively.

4.2.4. Apoptosis assay

To investigate the influence of compounds **9a**, **10h**, and **10k** on apoptosis, SKOV3 cells (10^6) were seeded in a six well plate and after 24 h incubation; cells were treated with 5 and 10 μM concentrations of compounds **9a**, **10h**, and **10k**. After 48 h incubation, cells were trypsinized and washed with cold PBS, and centrifuged at 3000 rpm. Then, the cells were mixed with binding buffer 5 μL of Annexin-V/FITC (Keygen Biotech, China) at room temperature for 15 min and then with PI solution (Keygen Biotech, China). The flow cytometric analysis of treated cells was conducted by using FACScan (Becton Dick-inson). The percentage of apoptotic cells was calculated using the excitation and emission settings of 488 nm and 535 nm (FL-1 channel); PI, 488 nm and 610 nm (FL-2 channel) [29].

4.3. Molecular docking studies

Molecular docking studies were performed for three promising compounds **9a**, **10h** and **10k**. Flexible-ligand docking procedure was performed by AutoDock 4 software (AutoDock Tools 1.5.6.) [30]. The crystal structure was taken from the protein data bank (PDB_ID: 4O2B). Chain D was selected for docking studies. The required hydrogen atoms, Kollman united atom charges and solvation parameters were added using the AutoDock Tools. The ligands were docked using the Lamarckian Genetic Algorithm (LGA) in the active site region. This region was defined through a grid map with 40, 40, and 40 grid points (X, Y, Z dimensions), that completely covers the space initially occupied by the crystallographic ligand. The centroid was selected as X = 17.0192, Y = 65.9939, Z = 43.3901. We used the default grid spacing (0.375 Å) and achieved 30 docking runs. The RMSD value of the ligand atoms in the re-docked and crystallographic conformations was 0.67. Figures of 2D and 3D presentations were created using ViewerLite and Discovery studio 3.0.

Acknowledgements

This project was supported by a grant (No. 2572) from the Research Council of Mazandaran University of Medical Sciences, Sari, Iran. This project was related to the Ph.D. thesis of MA (Pharmaceutical Sciences Research Center, Faculty of Pharmacy, Mazandaran University of Medical Sciences).

Appendix A. Supplementary material

Supplementary data to this article can be found online at https://doi.org/10.1016/j.bioorg.2019.103300.

References

[1] P. Anand, A.B. Kunnumakara, C. Sundaram, K.B. Harikumar, S.T. Tharakan, O.S. Lai, B. Sung, B.B. Aggarwal, Pharm. Res. 25 (2008) 2096–2216.
[2] K. Ahmad, M.K.A. Khan, M.H. Baig, M. Imran, G.K. Gupta, Anti-Cancer Agents Med. Chem. 18 (2018) 46–56.
[3] S. Ducki, G. Mackenzie, N.J. Lawrence, J.P. Snyder, J. Med. Chem. 48 (2005) 457–465.
[4] A.S. Negi, Y. Gautam, S. Alam, D. Chanda, S. Luqman, J. Sarkar, F. Khan, R. Konwar, Bioorg. Med. Chem. 23 (2015) 373–389.
[5] Y. Lu, J. Chen, M. Xiao, W. Li, D.D. Miller, Pharm. Res. 29 (2012) 2943–2971.
[6] D.L. Sackett, Pharmacol. Ther. 59 (1993) 163–228.
[7] H. Mirzaei, S. Emami, Eur. J. Med. Chem. 121 (2016) 610–639.
[8] L. Li, S. Jiang, X. Li, Y. Liu, J. Su, J. Chen, Eur. J. Med. Chem. 151 (2018) 482–494.
[9] G.C. Tron, T. Pirali, G. Sorba, F. Pagliai, S. Busacca, A.A. Genazzani, J. Med. Chem. 49 (2006) 3033–3044.
[10] D.K. Dalvie, A.S. Kalgutkar, S.C. Khojasteh-Bakht, R.S. Obach, J.P. O'Donnell, Chem. Res. Toxicol. 15 (2002) 269–299.
[11] R. Romagnoli, P.G. Baraldi, M.K. Salvador, F. Prencipe, V. Bertolasi, M. Cancellieri, A. Brancale, E. Hamel, I. Castagliuolo, F. Consolaro, E. Porcù, G. Basso, G. Viola, J. Med. Chem. 57 (2014) 6795–6808.
[12] D.A.E.M. Muhamad Mustafa, A.A. Mahmoud, A.M.G.O. Ibrahim, Eur. J. Med. Chem. 141 (2017) 293–305.
[13] Y.-H. Li, B. Zhang, H.-K.i. Yang, Q. Li, P.-C. Diao, W.-W. You, P.-L. Zhao, Eur. J. Med. Chem. 125 (2017) 1098–1106.
[14] M. Banimustafa, A. Kheirollahi, M. Safavi, S. Kabudanian Ardestani, H. Aryapour, A. Foroumadi, S. Emami, Eur. J. Med. Chem. 70 (2013) 692–702.
[15] S.M. Hashemi, H. Badali, H. Irannejad, M. Shokrzadeh, S. Emami, Bioorg. Med. Chem. 23 (2015) 1481–1491.
[16] S.M. Hashemi, H. Badali, M.A. Faramarzi, N. Samadi, M.H. Afsarian, H. Irannejad, S. Emami, Mol. Divers. 19 (2015) 15–27.
[17] J. van Meerloo, G.J. Kaspers, J. Cloos, Methods Mol. Biol. 731 (2011) 237–245.
[18] V. Pang, J. Yan, B. An, L. Huang, X. Li, Bioorg. Med. Chem 25 (2017) 3059–3067.
[19] H. Mirzaei, M. Shokrzadeh, M. Modanloo, A. Ziar, G.H. Riazi, S. Emami, Bioorg.

Chem. 75 (2017) 86–98.
[20] E. Gutierrez, J. Benites, J.A. Valderrama, P.B. Calderon, et al., Biochem. Biophys. Res. Commun. 466 (2015) 418–425.
[21] A. Rai, A. Surolia, D. Panda, PLoS One 7 (2012) e44311, , https://doi.org/10.1371/journal.pone.0044311.
[22] K.K. Gireesh, A. Rashid, S. Chakraborti, D. Panda, T. Manna, Biochem. Pharmacol. 84 (2012) 633–645.
[23] A. Kamal, G.B. Kumar, M.V. Vishnuvardhan, A.B. Shaik, V.S. Reddy, R. Mahesh, I.B. Sayeeda, J.S. Kapure, Org. Biomol. Chem. 13 (2015) 3963–3981.
[24] B. Zhang, Y.H. Li, Y. Liu, Y.R. Chen, E.S. Pan, W.W. You, P.L. Zhao, Eur. J. Med. Chem. 103 (2015) 335–342.
[25] R.C. Williams, J.C. Lee, Methods Enzymol. 85 (1982) 376–385.
[26] S.N. Timasheff, L.M. Grishman, Ann. Rev. Biochem. 49 (1980) 565–591.
[27] I.K. Lindamulage, H.Y. Vu, C. Karthikeyan, J. Knockleby, Y.F. Lee, P. Trivedi, H. Lee, Sci. Rep. 7 (2017) 10298, https://doi.org/10.1038/s41598-017-10972-0.
[28] A. Lambeirt, Y.A. Engelborghs, J. Biol. Chem. 256 (1981) 3279–3282.
[29] J.L. Browne, C. Gude, H. Rodriguez, R.E. Steele, A.J. Bhatnager, J. Med. Chem. 34 (1991) 725–736.
[30] G.M. Morris, R. Huey, W. Lindstrom, M.F. Sanner, R.K. Belew, D.S. Goodsell, J. Comput. Chem. 30 (2009) 2785–2797.